Journal of Polymer Research (2023) 30:434
https://doi.org/10.1007/s10965-023-03804-5

ORIGINAL PAPER

Ambidextrous polyanthracene/poly(ethylene glycol) copolymer for high capacity silicon anode in Li-ion batteries

Omer Suat Taskin[1,2] · Neslihan Yuca[2,3] · Joan Papavasiliou[4] · George Avgouropoulos[4] · Erhan Karabayir[5] · Mehmet Emre Cetintasoglu[1] · Emre Guney[2] · Ilknur Kalafat[2] · Busra Cetin[2] · Emre Guzel[6] · Osman Urper[7] · Kaiying Wang[7]

Received: 9 May 2023 / Accepted: 16 October 2023 / Published online: 4 November 2023

Abstract
The demand for lithium-ion batteries has dramatically increased in the last decade. However, the battery life offered by suppliers does not the level that can adequately meet the needs of end users. The development of new generation materials is so crucial accordingly. The nano-sized silicon with high theoretical capacity as the anode active material is one of the most promising sources, however, there are some problems (volume expansion) need to be solved in the use of silicon. In this study, a new generation polymer binder containing conjugated anthracene units, which gives conductivity and ethylene glycol lateral groups as another segment of the polymer backbone, which allows volumetric expansion with its flexibility has been developed. After preparing an electrode with silicon and developed conductive polymer binder (9:1) without adding any conductive additive, 800 mAh/g specific capacity is acquired after 400th cycle. It is thought that the obtained results will create an important infrastructure for the new generation conductive and flexible polymer binders for LIBs.

Keywords Anthracene · Ethylene glycol · Polymer binder · Conductive · LIBs

Introduction

Lithium-ion batteries (LIBs) have widespread using areas in electric vehicles, stationary applications, mobile devices like cell phones, notebooks, tablets, etc., owing to their considerable energy density. Graphite carbons are commonly used as the anode active material in commercial LIBs thanks to their acceptable cyclic performance and low costs. However, electrochemical performances of conventional graphite anodes are hard to meet the requirements of high energy batteries. Silicon anodes are one of the promising candidates for next-generation batteries, due to its low operating voltage (~0.37 V vs Li/Li$^+$), high theoretical capacity (4200 mAh/g at $Li_{22}Si_5$), environmental benign and abundant resources. Unfortunately, the utilization of silicon for negative electrode active material causes considerable changes in volume (>300%). During the lithiation/delithiation process, which is highly destructive for cycle stabilization, silicon anodes demonstrate rapid capacity fade. The mechanical stress caused by this repeated volume change pulverizes the anode compound and separates the LIBs components from each other as well as constantly increase the fractures that forming uncontrollable growth of solid electrolyte interphase (SEI)

✉ Omer Suat Taskin
omert@istanbul.edu.tr

1 Istanbul University, Institute of Marine Science and Management, Department of Chemical Oceanography, Vefa, 34134 Istanbul, Turkey

2 Enwair Energy Technologies Corporation, Maslak, 34469 Istanbul, Turkey

3 Istanbul Technical University, Energy Institute, Maslak, 34169, Sariyer, Istanbul, Turkey

4 Department of Materials Science, University of Patras, GR-265 04 Patras, Greece

5 Turkish Nuclear and Mineral Research Agency, Nuclear Energy Research Institute, TR34303, K. Cekmece, Istanbul, Turkey

6 Department of Engineering Fundamental Sciences, Sakarya University of Applied Sciences, 54050 Sakarya, Turkey

7 Faculty of Technology, Natural Sciences and Maritime Sciences Department of Microsystems Campus Vestfold, Nottoden, Norway

film, lead to in low Coulombic efficiency. This results in poor electrical contact between silicon particles and dreadful electrode degradation during the cycle [1–3]. Especially when the active material loading on electrodes is high these negative impacts become more apparent All these downsides could lead displeased cycling performance that hinders the practical application of silicon anodes [4, 5].

A silicon-based anode material is generally composed of a polymeric binder, silicon and carbon particles as active and conductive materials, respectively. Binders are used to connect the electrode components and many studies have been explored for enhancing the poor performance of the Si-based anode materials due to their abovementioned drawbacks [6–9]. Moreover, various alternatives such as carbon-coated and nano-sized silicon, porous composites, thin films, etc., have been put forward to get over these problems [10–13].

Unlike the graphite anodes composed of a layered structure to hold the lithium ions amongst the layers, silicon anodes alloy with lithium ions to form different phases of lithium silicates (Li_xSi) [14]. To overcome the abovementioned drawbacks of the volume changes in Si, various approaches have been developed [15, 16]. In recent years, the productivity of Si-Li electrode for developing of the polymer binding feature lots of endeavors have been conducted, supplying a flexible nature which enables silicon particles to spread along with the polymers in the silicon buffer medium and preserve the structure morphology. Majority of the commercial lithium-ion batteries (LIBs) are obtained from wet mixing of electrode active and conductive materials, polymer binder [17]. In the structure of the electrode, three factors diminish the volumetric and gravimetric energy concentration. After prolonged cycles, the connection between the conductive and electrode active materials will be broken due to the large volume changes during lithiation and the lack of binding strength of the conductive materials. Since delocalization of π-electrons and reduced or oxidized states, conjugated polymers (CP) have been one of the promising candidates for the conductive polymers [18–24]. Latest investigations on the features of organic CPs present an encouraging effect to tackle numerous issues of CPs thanks

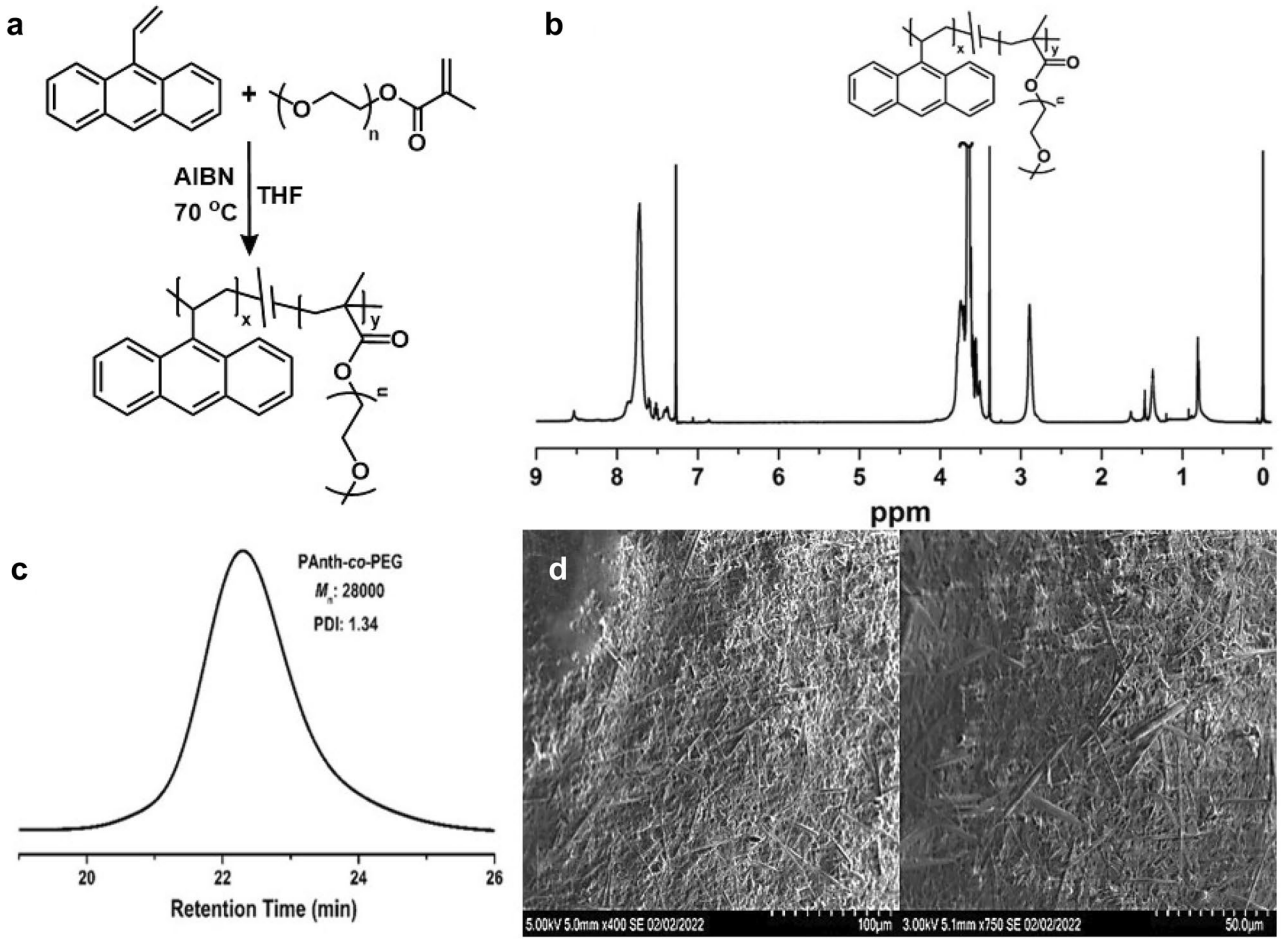

Fig. 1 Synthesis of PAnth-co-PEG via free radical polymerization (**a**), 1H-NMR spectrum of PAnth-co-PEG (**b**), GPC traces of PAnth-*co*-PEG (**c**), SEM images of PAnth-co-PEG in different magnifications (**d**)

to electronics, optics and biological technics [25–28]. Recent studies have concentrated on the significance of conductive and flexible polymeric binding agents to reduce the defects of silicon anodes. Moreover, self-healable polymeric binders have also been studied on by researchers over the last five years [20, 29–31]. The usage of proper binding agents like polyaniline (PANI), polyacrylic acid (PAA), etc., or block copolymers and supplementation of extra conductive carbon (which has an impact on energy density) silicon-based composite electrodes have been widely developed [32–40]. Biomass-derived polymers have been investigated to be as binders for LIBs in addition to their environmental applications [41–44]. The development of the conductive and flexible polymer binder has been previously reported by our group which is related to conductive fluorene-based main chain polymer [27]. Liu et al. indicated that polypyrene as a conjugated system and a triethylene group as a building block were used as a side group to make a conductive and flexible block copolymer [45]. However, pyrene is highly expensive and the low-chain part of ethylene glycol has a drawback for cycle life as well.

The drawbacks of the above-stated investigations can be resolved with longer chain poly(ethylene glycol) (PEG) as another segment of the main chain polymer. Here, the repeating ethylene oxide units in the side chains of PEG will considerably increase the polarity of the polymers, and the absorption of the electrolyte improves accordingly. Besides, the other advantage of the copolymer is that the binding strength and durability are improved to decrease stress-induced cracks. Briefly, the structural texture of the PAnth-*co*-PEG has great conjugation and conductivity characteristics and provides Si-based anode stability designed to append high levels of electronic conductivity, electrolyte absorption, and mechanical flexibility.

Results and discussion

According to our previous studies, it seemed appropriate to combine conjugated polymer structures with PEG units. Generally, conjugated polymers with benzene groups are obtained by free radical polymerization. ^{1}H-NMR spectral

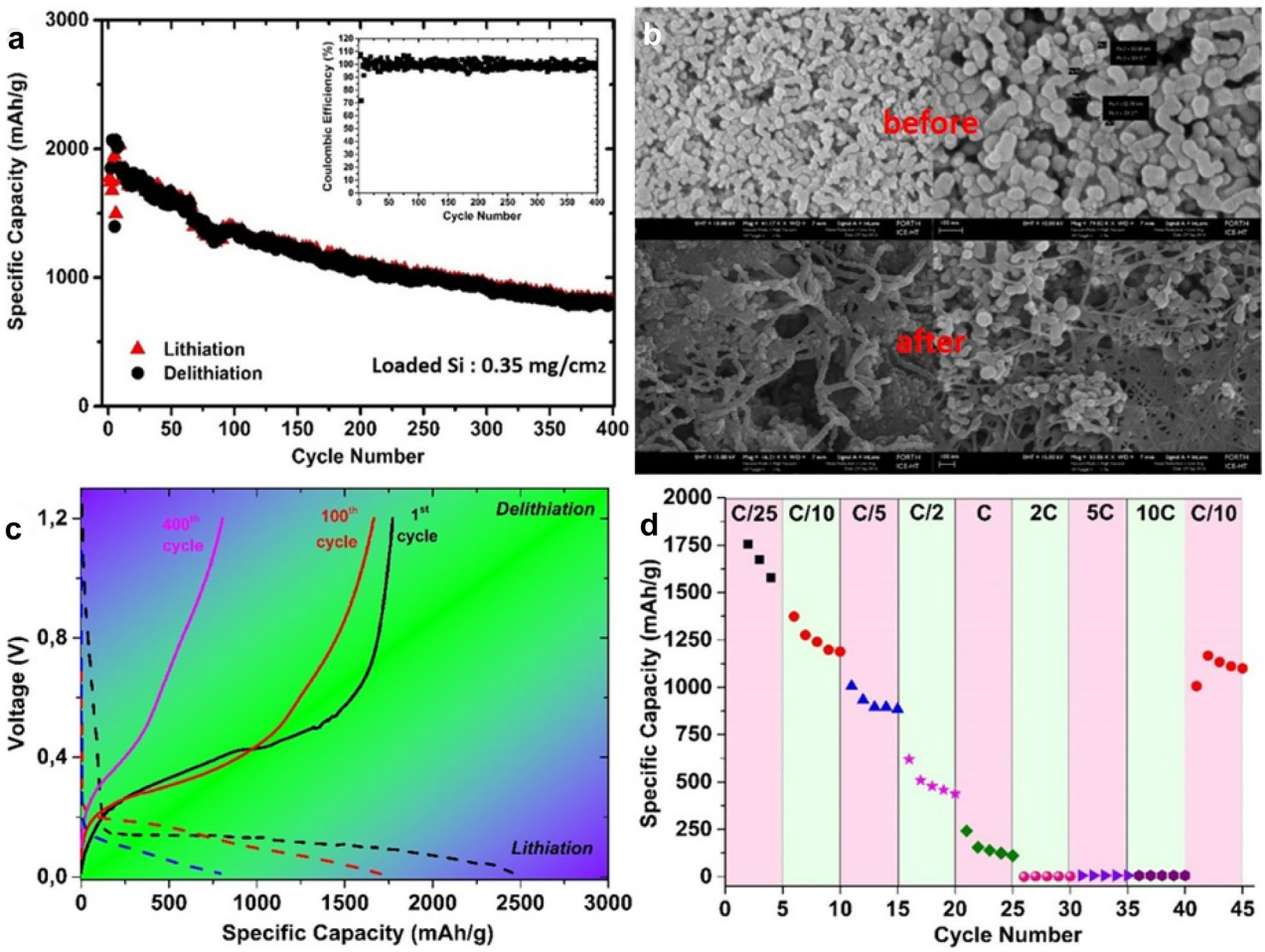

Fig. 2 Cycling data and coulombic efficiency of silicon electrode at C/3 (**a**), SEM images of electrodes at different magnification before cycling after 400th cycle (**b**), Voltage profile of Si electrode for 1st, 100th and 400th cycle (**c**), Cycling data of Si electrodes at different C-rates (**d**)

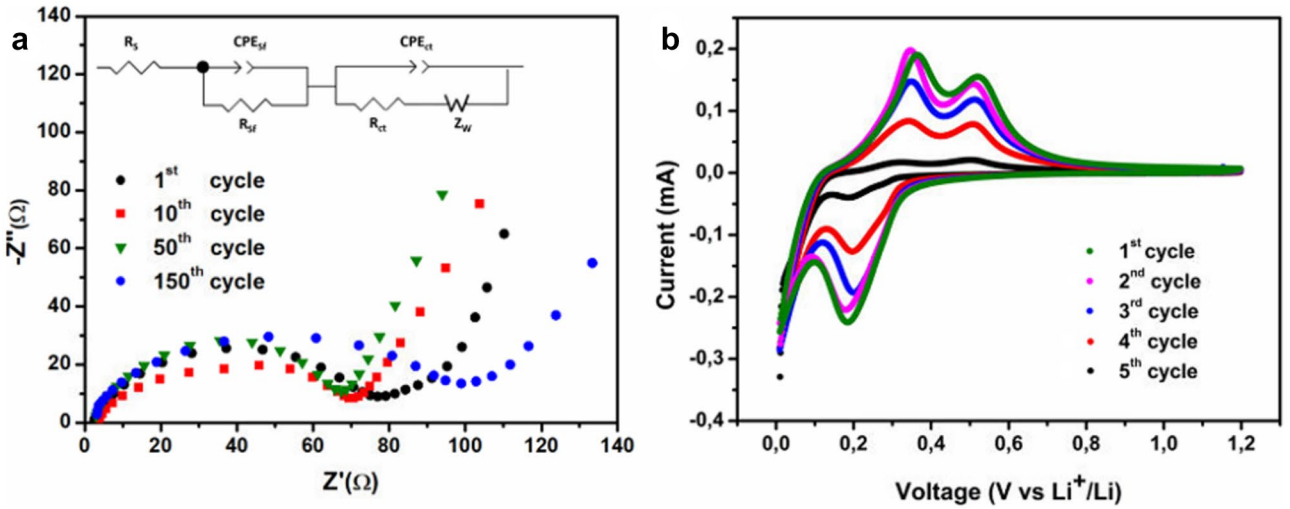

Fig. 3 The EIS results of cell at 1.2V with different cycles (**a**), CV curves of the electrode at a scan rate of 0.03 mV s-1 (**b**)

analysis of the construct proved the presence of both PEG repeating and benzene units. Picoammeter/Voltage Source and two ultra-pure platinum electrodes were used for the conductivity tests. The maximum conductivity of the PAnth-*co*-PEG was calculated as $1.33x10^{-4}$ S cm^{-1}.

The synthesis protocol of PAnth-*co*-PEG has been given in Fig. 1a. The structure of the copolymer was confirmed by ^{1}H NMR analysis as characteristic protons of both segments clearly were detected (Fig. 1b). The signal of aromatic protons at 7.3-7.9 ppm and the peak corresponding to etheric protons appearing at 3.66 ppm evidences the expected structure. Figure 1c shows the GPC trace of the PAnth-*co*-PEG. The GPC chromatogram of the copolymer displayed a unimodal distribution, showing no side reactions occurred during the reaction and proves the success of the coupling process. SEM images of PAnth-*co*-PEG which can be seen in Fig. 1d clearly display the PEG units as different size fiber in the polymer backbone.

Si nanoparticles pulverize during the lithiation-delithiation process due to the huge (300%) volume expansion of silicon. Si anode showed a specific capacity of 2485 mAh/g in the first cycle at C/3. After 400 cycles at the C/3 rate, the specific capacity decreased to 800 mAh/g, which equals 32.2% retention of the electrode capacity (Fig. 2a). The irreversible capacity loss of the electrode can be ascribed to pulverization of the active material and formation of SEI layers [40,41]. SEM images of the Si anode electrode before/after the 400^{th} cycle is shown in Fig. 2b. It can be seen in SEM images that Si particles are about lower than 50 nm before cycling, however, the particles expanded to 150-200 nm after cycling. The presence of the polymeric binder should support the formation of uniform Silicon/electrode coating on the copper foil, and the attained porous electrode may accommodate the volume change through the cycling process. With the help of poly (anthracene-polyethylene glycol) copolymer, it is clearly seen that some Si nanoparticles are prevented from being pulverized after 400 cycles. The loss of some of the Si particles causes a shortening of the lithiation-delithiation process and a decrease in the specific capacity of the electrode. Figure 2C demonstrates the characteristic discharge-charge curves of silicon anode at different cycles. The long plateaus beneath the 0.3 V through discharging of cell proposes continuous alloying reaction among Li and Si to form amorphous Li_xSi_y. The voltage plateau of the anode electrode shrank from cycle to cycle due to the pulverization of active materials (Fig. 2c). The capacitance of the Si anode at different C-rates showed in Fig. 2d and the initial cycle activated with C/25. From the electrochemical perspective, rate performance is implied to mean that a particular amount of specific charge is transferred while keeping a certain cell voltage limit. Under load, any resistance in the cell causes to a subsequent overvoltage, which reduces the operational voltage gap and decreases the attainable specific capacity [42]. Therefore, while the current density gradually ascended from C/25 to 10C, the Si anode with (PAnth-*co*-PEG) binder displayed low capacity with high C-rates (>1C). The Si anode continued to operate normally after returning from high C rates to low C rate (C/10). The C-rates of the Si anode demonstrated that the synthesized

Table 1 Rs, Rsf and Rct calculation of the electrode at 1^{st}, 10^{th}, 50^{th} and 150^{th} cycle on an equivalent circuit of the cell

Cycle no	Rs (Ω cm^2)	Rsf (Ω cm^2)	Rct (Ω cm^2)
1^{st}	2.46	79	32.2
10^{th}	3.68	70.6	32.98
50^{th}	2.97	67.4	36
150^{th}	3.21	98.56	35.58

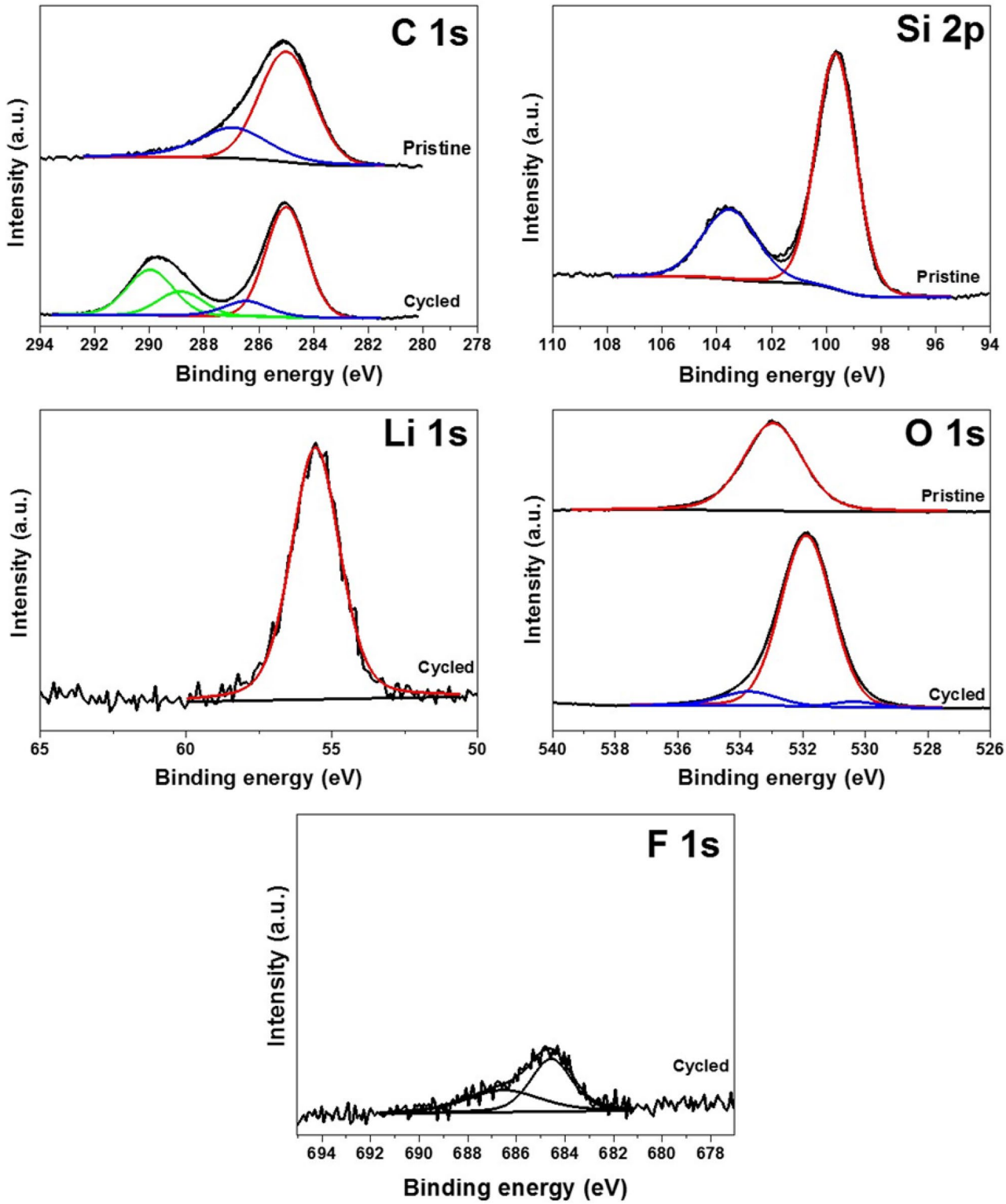

Fig. 4 XPS spectra of pristine and cycled Si/PAnth-*co*-PEG electrodes

(PAnth-*co*-PEG) binder was stable at operating voltage with different charging rates and maintains good integrity of the anode even at high current densities (Fig. 2d).

To get a better understanding of internal structure with ascending cycle numbers EIS analyses are carried out after first, 10^{th}, 50^{th} and 150^{th} cycles at 1.2 V over a frequency

range from 1 mHz to 100 kHz. Nyquist plots of the Si/PAnth-*co*-PEG are given in Fig. 3. The shift of impedance at Z0 axis implies the solvent resistance (Rs). The semicircle at high frequency region is ascribed to resistance of the surface including SEI and Si particles (Rsf). The slope in low frequency regions is associated to the solid-state diffusion of lithium-ion in the active material and charge transfer resistance (Rct). The equivalent circuit that fits the EIS plot of Si/PAnth-*co*-PEG electrode and its parameters are listed in Table 1. The EIS results indicate that impedance did not increase drastically within 50 cycles, demonstrating the formation of stable SEI layer. However, after 150 cycles Rsf and Rct value significantly increased due to the deterioration of SEI layer, leading the increased electrochemical impedance. The cyclic voltammetry curves at a scan speed of 0.3 mV s^{-1} also demonstrate the lithium insertion and desertion process. Two pairs of well-defined anodic peaks can be clearly observed at 0,36 V and 0,52 V and two cathodic peaks at 0,196 V and 0.06 V The two anodic peaks are ascribed to the disintegration of the lithiated phase $Li_{4.2}Si_{12}$ and to the complete extraction of lithium from the silicon [40]. First anodic peak detected in the CV measurements related to the phase transition from Phase-3 ($Li_{3.16}Si$) to Phase-2 (Li_7Si_3) and the second one is corresponded to the phase transition from the Phase-2 to the Phase-1 (LiSi) [43]. Regarding the cathodic side, there is no peak observed at 0.28 V which is related to the irreversible reaction of SiO_2 reduction [44]. The peaks at 0.21 V and at 0.06 V are commonly attributed to the insertion of lithium into the amorphous silicon structure.

Figures 4 shows the spectra corresponding respectively to C1s, Si2p, Li1s, O1s, and F1s core peaks at the surface of the pristine and cycled Si/PAnth-*co*-PEG electrodes. The presented XPS data has been compared with the results obtained by similar studies from the literature [3, 6]. Concerning silicon, the spectrum displays a first Si2p peak assigned to bulk silicon (~99.4eV red and black curves) before the cycle test and another one assigned to surface oxide SiO_2 (~103.5 eV, blue) after the cycle.

C1s spectrum shows several components. The narrow peak at ~287 eV (blue curve) corresponds to C-O bonds associated here with the carbon atoms. The main peak at 285 eV (red and black curves) is assigned to hydrocarbon surface contamination. O1s spectrum is composed of one major component at ~533 eV (red and black curves) associated with O environments in the C in the component for the pristine samples. This peak is observed to shift to lower binding energy due to the formation of carbonates (blue curves) in the SEI for the cycled samples.

The results indicate that no P is present in the pristine samples. LiF was detected in both cycled samples which resulted from the electrolyte. Particularly, in the cycled sample, a small peak at ~51.5eV (red and black curves) was observed associated with Li in an oxidized form after the cycle. The increase of the peak attributed to Li_2O both on O1s spectrum at ~533 eV (blue curve) as well as on Li1s spectrum at ~51.5 eV which is clearly visible for cycled electrodes. The absence of any other significant peak can be interpreted as the absence of the presence of Li compounds including Li_2CO_3 and lithium alkyl carbonates at the electrode surface. F1s spectra shows two F-containing components. LiF at ~684.5 eV (black curve) and another one at ~686 eV (black curve).

Conclusion

In a nutshell, PAnth-*co*-PEG was used as a conductive binder for high-capacity silicon anode for Li-ion battery application. The structural and electronic properties were investigated by spectroscopic and electrochemical techniques and the polymer/Si composite electrode exhibited excellent performance which is 800 mAh/g specific capacity after 400^{th} cycle without using any conductive additive. The obtained results will be developed to higher capacities and capacity retentions. Electrical and binding properties are enhanced without any effect to each other. Conductive and flexible polymer binders for LIBs will be one of the most promising materials as a crucial anode component in near future.

Supplementary Information The online version contains supplementary material available at https://doi.org/10.1007/s10965-023-03804-5.

Acknowledgement This work has been supported by Scientific Research Projects, Istanbul University with FYL-2018-33034 numbered project.

Funding Istanbul Üniversitesi, FYL-2018-33034, Omer Suat Taskin.

Data availability Data is available when it is requested.

Declarations

Conflict of interest All authors declare that they have no conflicts of interest.

References

1. Malik YT, Shin SY, Jang JI, Kim HM, Cho S, Do YR, Jeon JW (2023) Self-Repairable Silicon Anodes Using a Multifunctional Binder for High-Performance Lithium-Ion Batteries. Small 19(9):e2206141. https://doi.org/10.1002/smll.202206141
2. Yingqiang W, Xie L, Ming H, Guo Y, Hwang J-Y, Wenxi W, He X, Wang L, Alshareef H, Sun Y-K (2020) An Empirical Model for the Design of Batteries with High Energy Density. ACS Energy Lett. https://doi.org/10.1021/acsenergylett.0c00211
3. Yuca N, Taskin OS, Arici E (2020) An overview on efforts to enhance the Si electrode stability for lithium ion batteries. Energ Storage e94. https://doi.org/10.1002/est2.94
4. Zhang C, Chen Q, Ai X, Li X, Xie Q, Cheng Y, Kong H, Xu W, Wang L, Wang M-S, Yang H, Peng D-L (2020) Conductive polyaniline doped with phytic acid as a binder and conductive additive for a commercial silicon anode with enhanced lithium

storage properties. J Mater Chem A 8(32):16323–16331. https://doi.org/10.1039/D0TA04389C
5. Kwon HJ, Hwang JY, Shin HJ, Jeong MG, Chung KY, Sun YK, Jung HG (2020) Nano/Microstructured silicon-carbon hybrid composite particles fabricated with corn starch biowaste as anode materials for Li-ion batteries. Nano Lett 20(1):625–635. https://doi.org/10.1021/acs.nanolett.9b04395
6. Hu S, Wang L, Huang T, Yu A (2020) A conductive self-healing hydrogel binder for high-performance silicon anodes in lithium-ion batteries. J Power Sources 449:227472. https://doi.org/10.1016/j.jpowsour.2019.227472
7. Taskin OS, Yuca N, Papavasiliou J, Avgouropoulos G (2020) Interconnected conductive gel binder for high capacity silicon anode for Li-ion batteries. Mater Lett 273:127918. https://doi.org/10.1016/j.matlet.2020.127918
8. Li Z, Wu G, Yang Y, Wan Z, Zeng X, Yan L, Wu S, Ling M, Liang C, Hui KN, Lin Z (2022) An Ion-conductive grafted polymeric binder with practical loading for silicon anode with high interfacial stability in lithium-ion batteries. Adv Energy Mater 12(29):2201197. https://doi.org/10.1002/aenm.202201197
9. Li J, Wang Y, Xie X, Kong Z, Tong Y, Xu H, Xu H, Jin H (2022) A novel multi-functional binder based on double dynamic bonds for silicon anode of lithium-ion batteries. Electrochimica Acta 425:140620. https://doi.org/10.1016/j.electacta.2022.140620
10. Bulut E, Güzel E, Yuca N, Taskin OS (2020) Novel approach with polyfluorene/polydisulfide copolymer binder for high-capacity silicon anode in lithium-ion batteries. J Appl Polym Sci 137(4):48303. https://doi.org/10.1002/app.48303
11. Liu D, Zhao Y, Tan R, Tian LL, Liu Y, Chen H, Pan F (2017) Novel conductive binder for high-performance silicon anodes in lithium ion batteries. Nano Energy 36:206. https://doi.org/10.1016/j.nanoen.2017.04.043
12. Yang H, Jiang T, Zhou Y (2023) Enhanced lithium storage performance in si/mxene porous composites. Inorganics 11(7):279. https://doi.org/10.3390/inorganics11070279
13. Yu Y, Yang C, Jiang Y, Zhu J, Zhao Y, Liang S, Wang K, Zhou Y, Liu Y, Zhang J, Jiang M (2023) Sponge-like porous-conductive polymer coating for ultrastable silicon anodes in lithium-ion batteries. Small 2303779. https://doi.org/10.1002/smll.202303779
14. Sun Y, Liu K, Zhu Y (2017) Recent progress in synthesis and application of low-dimensional silicon based anode material for lithium ion battery. J Nanomater 2017:4780905. https://doi.org/10.1155/2017/4780905
15. Jiao X, Yin J, Xu X, Wang J, Liu Y, Xiong S, Zhang Q, Song J (2021) Highly energy-dissipative, fast self-healing binder for stable si anode in lithium-ion batteries. Adv Funct Mater 31(3):2005699. https://doi.org/10.1002/adfm.202005699
16. Kong X, Xi Z, Wang L, Zhou Y, Liu Y, Wang L, Li S, Chen X, Wan Z (2023) Recent progress in silicon−based materials for performance−enhanced lithium−ion batteries. Molecules 28(5):2079. https://doi.org/10.3390/molecules28052079
17. Gao S, Sun F, Brady A, Pan Y, Erwin A, Yang D, Tsukruk V, Stack AG, Saito T, Yang H, Cao P-F (2020) Ultra-efficient polymer binder for silicon anode in high-capacity lithium-ion batteries. Nano Energy 73:104804. https://doi.org/10.1016/j.nanoen.2020.104804
18. Qi Y, Hien N, Oh E-S (2020) Enhancement of the lithium titanium oxide anode performance by the copolymerization of conductive polypyrrole with poly(acrylonitrile/butyl acrylate) binder. J Appl Electrochem 50. https://doi.org/10.1007/s10800-020-01401-8
19. Wu Z, Wan Z, Li Z, Du Q, Wu T, Cao J, Ling M, Liang C, Tan Y (2023) Partially carbonized polymer binder with polymer dots for silicon anodes in lithium-ion batteries. Small 19(2):2205065. https://doi.org/10.1002/smll.202205065
20. Nam J, Kim E, K.K R, Kim Y, Kim T-H (2020) A conductive self healing polymeric binder using hydrogen bonding for Si anodes in lithium ion batteries. Sci Rep 10(1):14966. https://doi.org/10.1038/s41598-020-71625-3
21. Mery A, Bernard P, Valero A, Alper J, Herlin-Boime N, Haon C, Duclairoir F, Sadki S (2019) A polyisoindigo derivative as novel n-type conductive binder inside Si@C nanoparticle electrodes for Li-ion battery applications. J Power Sources 420:9–14. https://doi.org/10.1016/j.jpowsour.2019.02.062
22. Su Y, Feng X, Zheng R, Lv Y, Wang Z, Zhao Y, Shi L, Yuan S (2021) Binary network of conductive elastic polymer constraining nanosilicon for a high-performance lithium-ion battery. ACS Nano 15(9):14570–14579. https://doi.org/10.1021/acsnano.1c04240
23. Yang Y, Wu S, Zhang Y, Liu C, Wei X, Luo D, Lin Z (2021) Towards efficient binders for silicon based lithium-ion battery anodes. Chem Eng J 406:126807. https://doi.org/10.1016/j.cej.2020.126807
24. Liu X, Zai J, Iqbal A, Chen M, Ali N, Qi R, Qian X (2020) Glycerol-crosslinked PEDOT:PSS as bifunctional binder for Si anodes: Improved interfacial compatibility and conductivity. J Colloid Interface Sci 565:270–277. https://doi.org/10.1016/j.jcis.2020.01.028
25. Tasdelen MA, Taskin OS, Celik C (2016) Orthogonal synthesis of block copolymer via photoinduced cuaac and ketene chemistries. Macromol Rapid Commun 37(6):521–526. https://doi.org/10.1002/marc.201500563
26. Xu G, Qb Yan, Kushima A, Zhang X, Pan J, Li J (2017) Conductive graphene oxide-polyacrylic acid (GoPAA) binder for lithium-sulfur battery. Nano Energy 31:568. https://doi.org/10.1016/j.nanoen.2016.12.002
27. Yuca N, Cetintasoglu ME, Dogdu MF, Akbulut H, Tabanli S, Colak U, Taskin OS (2018) Highly efficient poly(fluorene phenylene) copolymer as a new class of binder for high-capacity silicon anode in lithium-ion batteries. Int J Energy Res 42(3):1148–1157. https://doi.org/10.1002/er.3913
28. Wang F, Ma X, Li Y, Liu H, Wu Q, Guan X, Liu H, Wang X (2023) Room-temperature rapid self-healing polymer binders for si anodes in highly cycling-stable and capacity-maintained lithium-ion batteries. ACS Appl Energy Mater 6. https://doi.org/10.1021/acsaem.3c00161
29. Qin J, Lin F, Hubble D, Wang Y, Li Y, Murphy IA, Jang S-H, Yang J, Jen AKY (2019) Tuning self-healing properties of stiff, ion-conductive polymers. J Mater Chem A 7(12):6773–6783. https://doi.org/10.1039/C8TA11353J
30. Taskin OS, Kiskan B, Yagci Y (2013) Polybenzoxazine precursors as self-healing agents for polysulfones. Macromolecules 46(22):8773–8778. https://doi.org/10.1021/ma4019153
31. Yuca N, Kalafat I, Guney E, Cetin B, Taskin OS (2022) Self-healing systems in silicon anodes for Li-ion batteries. Materials 15(7):2392. https://doi.org/10.3390/ma15072392
32. Taskin OS, Kiskan B, Weber J, Yagci Y (2015) One-pot, one-step strategy for the preparation of clickable melamine based microporous organic polymer network. Macromol Mater Eng 300(11):1116–1122. https://doi.org/10.1002/mame.201500123
33. Taskin OS, Temel BA, Tasdelen MA, Yagci Y (2015) Synthesis of block copolymers by selective H-abstraction and radical coupling reactions using benzophenone/benzhydrol photoinitiating system. Eur Polym J 62:304–311. https://doi.org/10.1016/j.eurpolymj.2014.07.007
34. Zhao H, Wei Y, Qiao R, Zhu C, Zheng Z, Ling M, Jia Z, Bai Y, Fu Y, Lei J (2015) Conductive polymer binder for high-tap-density nanosilicon material for lithium-ion battery negative electrode application. Nano Lett 15:7927. https://doi.org/10.1021/acs.nanolett.5b03003
35. Zheng H, Yang R, Liu G, Song X, Battaglia VS (2012) Cooperation between active material, polymeric binder and conductive carbon additive in lithium ion battery cathode. J Phys Chem C 116:4875. https://doi.org/10.1021/jp208428w
36. Güzel E, Koçyiğit ÜM, Taslimi P, Erkan S, Taskin OS (2021) Biologically active phthalocyanine metal complexes: Preparation,

evaluation of α-glycosidase and anticholinesterase enzyme inhibition activities, and molecular docking studies. JBMT 35(6):e22765. https://doi.org/10.1002/jbt.22765
37. Tanaka S, Narutomi T, Suzuki S, Nakao A, Oji H, Yabuuchi N (2017) Acrylonitrile-grafted poly (vinyl alcohol) copolymer as effective binder for high-voltage spinel positive electrode. J Power Sources 358:121. https://doi.org/10.1016/j.jpowsour.2017.05.032
38. Tong Y, Jin S, Xu H, Li J, Kong Z, Jin H, Xu H (2023) An energy dissipative binder for self-tuning silicon anodes in lithium-ion batteries. Advanced Science 10(2):2205443. https://doi.org/10.1002/advs.202205443
39. Xu Z, Chu X, Wang K, Zhang H, He Z, Xie Y, Yang W (2023) Stress-dissipated conductive polymer binders for high-stability silicon anode in lithium-ion batteries. J Mater 9(2):378–386. https://doi.org/10.1016/j.jmat.2022.09.013
40. Heubner C, Nikolowski K, Reuber S, Schneider M, Wolter M, Michaelis A (2021) Recent insights into rate performance limitations of Li-ion Batteries. Batteries & Supercaps 4(2):268–285. https://doi.org/10.1002/batt.202000227
41. Ryu J, Kim S, Kim J, Park S, Lee S, Yoo S, Kim J, Choi N-S, Ryu J-H, Park S (2020) Room-Temperature crosslinkable natural polymer binder for high-rate and stable silicon anodes. Adv Funct Mater 30(9):1908433. https://doi.org/10.1002/adfm.201908433
42. Taskin OS, Hubble D, Zhu T, Liu G (2021) Biomass-derived polymeric binders in silicon anodes for battery energy storage applications. Green Chem. 23(20):7890–7901. https://doi.org/10.1039/D1GC01814K
43. Taskin OS, Kiskan B, Aksu A, Balkis N, Yagci Y (2016) Copper(II) removal from the aqueous solution using microporous benzidine-based adsorbent material. J Environ Chem Eng. 4(1):899–907. https://doi.org/10.1016/j.jece.2015.12.041
44. K K R, Jang W, Kim S, Kim T-H (2022) Chitosan- grafted -gallic acid as a nature-inspired multifunctional binder for high-performance silicon anodes in lithium-ion batteries. ACS Appl Energy Mater 5. https://doi.org/10.1021/acsaem.1c03791
45. Park SJ, Zhao H, Ai G, Wang C, Song X, Yuca N, Battaglia VS, Yang W, Liu G (2015) Side-chain conducting and phase-separated polymeric binders for high-performance silicon anodes in lithium-ion batteries. J Am Chem Soc 137:2565. https://doi.org/10.1021/ja511181p